

# Learning Motion Blur Robust Vision Transformers for Real-Time UAV Tracking

You Wu<sup>a</sup>, Xucheng Wang<sup>b</sup>, Dan Zeng<sup>c</sup>, Hengzhou Ye<sup>a</sup>, Xiaolan Xie<sup>a</sup>, Qijun Zhao<sup>d</sup>, Shuiwang Li<sup>a,\*</sup>

<sup>a</sup>*College of Computer Science and Engineering, Guilin University of Technology, Guilin, 541004, China*

<sup>b</sup>*School of Computer Science, Fudan University, Shanghai, 200082, China*

<sup>c</sup>*School of Artificial Intelligence, Sun Yat-sen University, Zhuhai, 510275, China*

<sup>d</sup>*College of Computer Science, Sichuan University, Chengdu, 610065, China*

---

## Abstract

Unmanned aerial vehicle (UAV) tracking is critical for applications like surveillance, search-and-rescue, and autonomous navigation. However, the high-speed movement of UAVs and targets introduces unique challenges, including real-time processing demands and severe motion blur, which degrade the performance of existing generic trackers. While single-stream vision transformer (ViT) architectures have shown promise in visual tracking, their computational inefficiency and lack of UAV-specific optimizations limit their practicality in this domain. In this paper, we boost the efficiency of this framework by tailoring it into an adaptive computation framework that dynamically exits Transformer blocks for real-time UAV tracking. The motivation behind this is that tracking tasks with fewer challenges can be adequately addressed using low-level feature representations. Simpler tasks can often be handled with less demanding, lower-level features. This approach allows the model use computational resources more efficiently by focusing on complex tasks and conserving resources for easier ones. Another significant enhancement introduced in this paper is the improved effectiveness of ViTs in handling motion blur, a common issue in UAV tracking caused by the fast movements of either the UAV, the tracked objects, or both. This is achieved by acquiring motion blur robust representations through enforcing invariance in the feature representation of

---

\*Corresponding author

*Email address:* lishuiwang0721@163.com (Shuiwang Li)

the target with respect to simulated motion blur. We refer to our proposed approach as BDTrack. Extensive experiments conducted on four tracking benchmarks validate the effectiveness and versatility of our approach, demonstrating its potential as a practical and effective approach for real-time UAV tracking. Code is released at: <https://github.com/wuyou3474/BDTrack>.

*Keywords:* UAV tracking, real-time, Vision Transformer, dynamic early exiting, motion blur robust representations

---

## 1. Introduction

In recent years, Artificial Intelligence (AI) has brought transformative progress across various domains, including AI-driven models [1, 2], multi-modal learning [3, 4], dynamic resource allocation [5, 6], unmanned aerial vehicle (UAV) tracking [7, 8, 9], and intelligent energy systems and control applications [10, 11, 12, 13, 14, 15, 16]. Recent advancements have broadly improved system performance, energy efficiency, and real-time decision-making across various engineering fields. These developments have motivated us to apply them to UAV tracking, aiming to improve accuracy, enhance robustness in dynamic environments, and achieve efficient real-time processing. UAV tracking involves the process of determining and predicting the location and size of a specific object in successive aerial images. This capability has become increasingly essential in a variety of fields, such as public safety, environmental monitoring, industrial inspections, disaster relief, and agriculture, due to its wide-ranging applications and benefits [7, 17, 9, 18, 19, 20]. These applications present unique challenges, including the need for accurate tracking in resource-constrained environments, where UAVs often face limited battery life and computational resources. Therefore, efficient tracking algorithms that ensure sustained and accurate performance under these conditions are paramount [8, 21]. Traditional discriminative correlation filter (DCF)-based trackers have been widely used in UAV tracking due to their efficiency [22, 23, 24, 25]. However, their tracking precision often falls behind that of deep learning (DL)-based methods, which have shown promising results in terms of precision [17, 8, 18, 19]. Despite the advantages of DL-based methods, they face significant challenges in real-time applications, especially in resource-limited scenarios, where both computational power and battery life are constrained. Recent advances in the tracking community have led to the emergence of single-stream architectures, particularly those leveraging

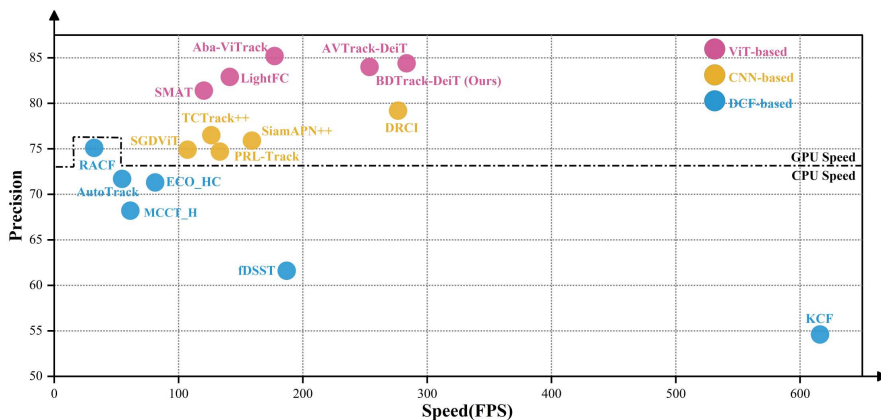


Figure 1: Compared with state-of-the-art UAV tracking algorithms on four UAV tracking benchmarks, our BDTrack-DeiT sets a new record with 0.844 precision while maintaining efficient performance at around 283 FPS.

pre-trained vision transformer (ViT) backbone networks. These architectures have demonstrated notable success in integrating feature extraction and correlation [26, 27, 28, 29]. In line with this trend, Aba-ViTrack [9] introduces an efficient DL-based tracker that adopts a single-stream ViT framework with adaptive token selection, achieving a good balance between precision and speed. However, its variable token scheme incurs unstructured access overhead. Motivated by this, we adopt a similar architecture but enhance efficiency through a structured early exiting strategy.

Early exiting is a technique designed to expedite the processing of input data by allowing a model to terminate its forward pass prematurely based on certain criteria, reducing computational costs without compromising much predictive accuracy, especially if the behavior or characteristics of the task vary based on the specific examples or instances involved. While previous research has mainly explored this idea in domains such as natural language processing and image classification [30, 31, 32, 33, 6, 34], visual tracking, particularly real-time UAV tracking, poses unique challenges that differentiate it from these static tasks. Unlike image classification, visual tracking requires maintaining temporal consistency across frames, coping with abrupt target motion, deformation, scale variation, and appearance changes. These properties demand early-exit strategies that not only assess the model’s confidence for a single frame but also account for the temporal dependency of predictions and the evolving target appearance over time. Existing studies

have investigated diverse strategies, including adaptive confidence-based exits [30, 6], distillation [35], architectural design [36, 32], and specialized training schemes [31, 33], applied to architectures ranging from convolutional neural networks (CNNs) [30, 35] to recurrent neural networks (RNNs) [36] and Transformers [32, 6]. While these methods have shown success in applications such as NLP [36, 33], image classification [6], video recognition [37], image captioning [38], and vision-language learning [5], their direct application to UAV tracking remains largely unexplored. This gap motivates our work, which adapts early-exit mechanisms to the real-time, temporally dependent, and appearance-variant nature of UAV tracking.

In addition, this research also aims to enhance the performance of UAV trackers by mitigating the adverse effects of motion blur, which is a prevalent challenge in UAV tracking as rapid and unpredictable movements of UAVs are common due to factors such as wind, changes in altitude, sudden maneuvers, or the need to track fast-moving targets [24, 21, 39]. For example, existing trackers [17, 8] show a marked increase in center location error (CLE) during real-world testing with motion-blurred sequences, rising from under 10 pixels to over 20, a threshold commonly regarded as tracking failure. This degradation becomes especially severe during aggressive UAV maneuvers such as sharp turns or rapid accelerations, where motion blur is significantly intensified, further impairing tracking performance. Although numerous methods have been proposed to address motion blur in visual tracking [40, 41, 42, 43, 44], their practical use in real-time UAV tracking remains limited due to inherent shortcomings. In contrast, we propose to learn motion blur robust feature representations with ViTs by minimizing the mean square error (MSE) between the feature representation of the original template and its blurred version subject to motion blur. Our approach distinguishes itself through its simplicity, avoiding the inclusion of extra architectural complexities. The proposed framework is called BDTrack. Validation using real-world data demonstrates that our method significantly enhances the robustness against motion blur of baseline methods. Remarkably, our BDTrack-DeiT outperforms the SOTA tracker ABDNet [44], which was proposed to address motion blur, by 5.5% in precision on the motion blur subset of the UAVDT dataset with more than 2 times faster GPU speed (See Fig. 4 and Table 1). Extensive experiments on four benchmarks show that our method achieves SOTA performance. As shown in Fig. 1, our method sets a new record with a average precision of 0.844 and runs efficiently at around 283 frames per second (FPS) on the four UAV tracking benchmarks. Its real-time, motion-blur-robust tracking

improves UAV efficiency in applications such as agricultural inspection by enabling faster and wider-area coverage with minimal computational load, and in disaster relief operations by maintaining reliable tracking in challenging conditions to support quicker and more effective search-and-rescue missions. We also emphasize its suitability for resource-constrained UAVs through adaptive computation that preserves battery life and processing power.

The following is a summary of our contributions:

- We introduce a novel module that adaptively streamlines the architecture of ViTs by dynamically exiting Transformer blocks. Our method is straightforward and can significantly enhance the efficiency of baseline ViT-based UAV tracking methods with minimal impact on their tracking performance.
- We make a pioneering effort to enhance the motion blur robustness of vision transformers (ViTs) for real-time UAV tracking by leveraging a simple mean square error (MSE) loss to enforce feature invariance of the target under simulated blur. Our approach incurs no additional computational burden during the inference, making it well-suited for real-time UAV tracking.
- We present BDTrack, an efficient tracker seamlessly integrating these components, which is readily integrable into similar ViT-based trackers. BDTrack is able to maintain high tracking speeds while delivering exceptional performance. Extensive experiments on four benchmarks confirm its state-of-the-art performance.

## 2. Related Work

### 2.1. Motion Blur Aware Trackers

Motion blur presents a significant challenge in visual tracking, and various approaches have been proposed to address this issue and enhance the robustness of tracking algorithms [45, 41, 42, 43, 44], including employing specialized architectures or mechanisms to handle motion blur, learning motion blur robust representations, and combining motion deblurring techniques. For example, Ding et al. [45] introduce a method to enhance the robustness of the appearance model against severe blur by incorporating various blur kernels during the training process. Guo et al. [43] propose a novel generative adversarial network (GAN)-based scheme aimed at enhancing tracker

robustness to motion blurs. To address the challenges posed by motion blur in UAV tracking, Zuo et al. [44] introduced the tracking-oriented adversarial blur-deblur network (ABDNet) very recently, which includes a novel deblurring component to restore the visual appearance of blurred targets and an innovative blur generator that creates realistic blurry images for adversarial training. However, existing methods for handling motion blur often involve complex architectures [46, 44] or training pipelines [42, 44] and neglect runtime efficiency [40, 41, 43], limiting their suitability for UAV applications. We introduce motion blur robust ViTs for UAV tracking that learn invariant feature representations efficiently without adding inference overhead, making them ideal for real-time scenarios. The method is easily adaptable to other ViT-based trackers, improving performance under motion blur without sacrificing speed.

## 2.2. Efficient Vision Transformers

Efforts to enhance the efficiency of ViTs have garnered significant attention in recent years, driven by the need to reconcile their powerful representation capabilities with computational efficiency. One avenue of exploration involves the design of lightweight ViT architectures, employing techniques such as low-rank methods, model compression, and hybrid designs [47, 48, 49]. However, low-rank and quantization-based ViTs often trade substantial accuracy for efficiency gains. Pruning-based ViTs typically require intricate decisions on pruning ratios and involve a time-consuming fine-tuning process. Hybrid ViTs featuring CNN-based stems impose limitations on input size flexibility, preventing the simultaneous input of images with varying dimensions [9].

Conditional computation-based ViTs have recently enabled adaptive inference by dynamically adjusting computation based on input complexity [50, 51]. For example, A-ViT [51] eliminates extra halting networks via ACT-like mechanisms, improving both efficiency and accuracy. A-ViTTrack [9] extends this design to UAV tracking, but suffers from the overhead of unstructured token selection. In contrast, our DEEM adopts a structured early-exit strategy that enables efficient inference, implemented using only a simple linear layer with sigmoid activation. Nevertheless, existing studies primarily focus on large-scale models and incorporate inefficient architectures or training methods for making early exiting decisions [33, 38, 5, 6]. These criteria for early exiting are challenging to adapt effectively to lightweight models. For example, the early exiting strategy proposed for vision language models in [5] relies on layer-wise cosine similarities. While cosine similarities have proven effective

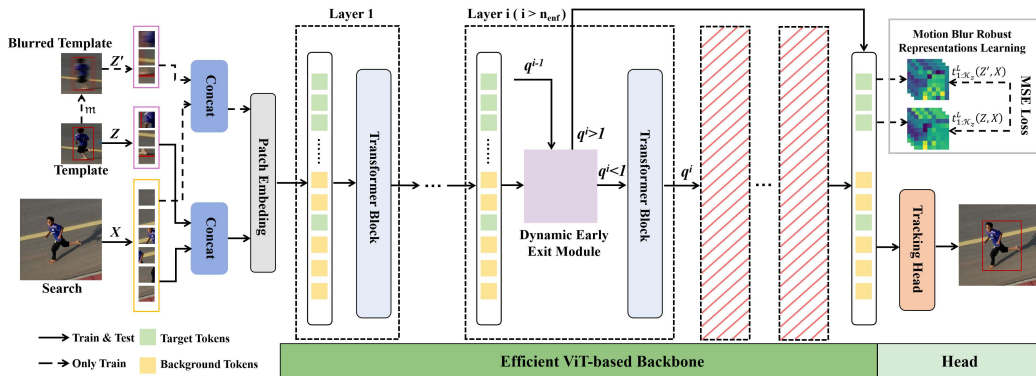


Figure 2: Overview of the proposed BDTrack. It comprises of a single-stream backbone and a prediction head. MBRV and DEEM (see Fig. 3) are employed to learn motion blur robust representations and to boost efficiency, respectively. Note that  $m$  applies simulated motion blur to the template image  $Z$  using the method from [54]. DEEM takes a subset of tokens from the target template and search image as input, outputting the exit score (i.e.,  $q$ ) at the corresponding ViT block.

for large-scale models characterized by high-level and high-dimensional feature representations, their performance may be suboptimal in lightweight models where non-linearities and complex dependencies are challenging to linearize or trivialize [52, 53]. The dynamic early exiting method proposed for accelerating ViTs in [6] involves training delicate Local Perception and Global Aggregation Heads separately with distinct supervisions. However, this intricate training setup introduces significant inefficiencies into the training process. In this work, we explore a more structured and efficient approach to dynamically early exit ViT blocks by incorporating a dynamic early exit module. Our method aims to simplify the training process, improve inference efficiency, and maintain adaptability across different ViT-based models.

### 3. Method

In this section, we first briefly overview our tracking framework, BDTrack, as illustrated in Fig. 2. Then, we introduce the proposed method for learning motion blur robust ViTs (MBRV) and the dynamic early exit module (DEEM). Finally, we detail the prediction head and training objective.

#### 3.1. Overview

Our BDTrack is a tracking framework that employs a single-stream approach, taking the target template and the search image as inputs. This

framework consists of an adaptive ViT-based backbone and a prediction head. The features extracted from the backbone are subsequently forwarded to the prediction head to achieve tracking predictions. To enhance the robustness of ViTs against motion blur, we minimize the mean squared error (MSE) between the feature representations of the target template and its blurred counterpart. The blurred version of the template is generated using the linear motion blur method, as referenced in [55]. This approach aims to ensure that the ViTs can maintain consistent performance even when the input images are affected by motion blur, a common issue in UAV tracking. Additionally, to further enhance the efficiency of ViTs, we introduce a dynamic early exit module (DEEM) for each ViT block (layer), excluding the initial  $n_{enf}$  blocks. This module is trained to dynamically predict the exiting score  $\epsilon^l$  at the  $l$ -th layer. The forward pass of the ViT exists at layer  $l$  when the cumulative exiting score exceeds a certain threshold. This mechanism allows the model to allocate computational resources more efficiently, exiting early for simpler tasks and reserving full processing power for more complex ones. The details of the two components will be elaborated in the subsequent subsections.

### 3.2. Learning Motion Blur Robust ViTs (MBRV)

A motion blur robust ViT (MBRV) serves as a pivotal component in our pursuit of a compact and efficient end-to-end tracker specifically designed for real-time UAV tracking. In the context of UAV tracking, where rapid and accurate object localization is paramount, the presence of motion blur in captured images poses a significant challenge. Motion blur can distort object features, leading to inaccuracies in tracking algorithms and potentially compromising the effectiveness of the entire tracking system. The inclusion of MBRV addresses these challenges by ensuring that the ViT-based backbone of our tracking system remains effective even in the presence of motion blur. By minimizing the Mean Squared Error (MSE) between the feature representations of the target template and its blurred counterpart, MBRV enhances the robustness of the tracker. Furthermore, the compact and efficient nature of MBRV aligns with our goal of developing a tracker optimized for real-time UAV tracking. It is worthy of note that we choose to blur the template patch rather than the search patch is based on the following considerations: 1) It allows a controllable blurring of the target, as the object in the template always is sharp and unblurred while the object in the search patch is frequently subject to motion blur. 2) Since the size of the template patch and the scale of the target are fixed, the tokens associated with the

template can be precisely identified. But the identification of the objects in the search patch may involve interpolation due to translation and scale variations of the objects. As the size of the search patch is fixed, interpolation has to be conducted on the feature space. However, interpolating in the feature space can lead to several issues, including loss of spatial information, misalignment of features, and inconsistent semantic meaning. These factors can result in poorer quality interpolated features, affect training dynamics, and potentially lead to suboptimal model performance.

During the training phase, the MBRV receives three inputs: a target template  $Z$ , a blurred target template  $Z' = \mathbf{m}(Z)$ , and a search image  $X$ , where  $\mathbf{m}(Z)$  represents applying simulated motion blur to the template image  $Z$  using the linear motion blur method implemented in [54]. The input images are first segmented and then flattened into sequences of patches. Subsequently, the sequences corresponding to  $Z$  and  $X$  are concatenated into an ordered sequence denoted by  $[Z, X]$ . The same procedure is applied to the sequences corresponding to  $Z'$  and  $X$ , leading to  $[Z', X]$ . In the forward pass,  $[Z, X]$  is tokenized by a trainable linear projection layer  $\mathcal{E}$  called patch embedding, which generates  $\mathcal{K}$  tokens as follows:

$$\mathbf{t}_{1:\mathcal{K}}^0 = \mathcal{E}([Z, X]) \in \mathbb{R}^{\mathcal{K} \times d}, \quad (1)$$

where the embedding dimension of each token is denoted by  $d$ , and the token sequences  $t_{1:\mathcal{K}_z}^0$  and  $t_{\mathcal{K}_z+1:\mathcal{K}}^0$  ( $1 < \mathcal{K}_z < \mathcal{K}_x < \mathcal{K}$ ) correspond to the template and search image, respectively, where  $\mathcal{K} = \mathcal{K}_z + \mathcal{K}_x$ . The  $\mathcal{K}$  tokens  $\mathbf{t}_{1:\mathcal{K}}^0$  are then input into the Transformer blocks to obtain their final feature representations. Let  $\mathfrak{T}^l$  represent the Transformer block at layer  $l$ , transforming all tokens from layer  $(l - 1)$  as  $\mathbf{t}_{1:\mathcal{K}}^l = \mathfrak{T}^l(\mathbf{t}_{1:\mathcal{K}}^{l-1})$ . The overall MBRV of  $L$  ViT blocks in total, denoted by  $\mathfrak{B}$ , can be expressed as:

$$\mathbf{t}_{1:\mathcal{K}}^L(Z, X) = \mathfrak{B}(Z, X) = \mathfrak{T}^L \circ \mathfrak{T}^{L-1} \circ \dots \circ \mathfrak{T}^1 \circ \mathcal{E}([Z, X]), \quad (2)$$

where  $\circ$  denotes the composition operation. Similarly, we can derive the feature representation of  $[Z', X]$ . As  $[Z, X]$  and  $[Z', X]$  are ordered sequences of tokens, the feature representation of  $Z$  and  $Z'$  can be retrieved by tracking their token indices in the respective ordered sequences, specifically denoted as  $\mathbf{t}_{1:\mathcal{K}_z}^L(Z, X)$  and  $\mathbf{t}_{1:\mathcal{K}_z}^L(Z', X)$ , respectively. The core idea behind MBRV is to minimize the mean square error between the feature representation of  $Z$  and that of  $Z'$ . This is achieved by minimizing the following MSE loss:

$$\mathcal{L}_{br} = \|\mathbf{t}_{1:\mathcal{K}_z}^L(Z, X) - \mathbf{t}_{1:\mathcal{K}_z}^L(Z', X)\|^2. \quad (3)$$

During the inference phase, only the sequence  $[Z, X]$  is input to the MBRV, there is no need for simulating motion blur. Consequently, our method does not introduce any additional computational cost in the inference phase. Notably, our method is agnostic to the specific ViTs employed, allowing seamless integration with any ViTs within our framework.

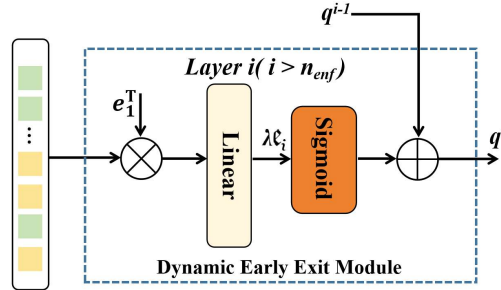


Figure 3: The detailed structure of the DEEM. The variables  $\mathbf{e}_1^T$  represents a subset of all tokens output by the  $(i-1)$ -th ViT block,  $\ell_i$  denotes the exit score of the  $i$ -th Transformer block, Sigmoid represents the sigmoid function, and  $q^i$  denotes the cumulative exit score before  $(i-1)$ .

### 3.3. Dynamic Early Exit Module (DEEM)

The primary goal of the DEEM is to allocate computational resources in a dynamic manner based on the complexity of each ViT block’s input, aiming to enhance inference efficiency while preserving performance. The DEEM operates by dynamically assessing the complexity of the input at each ViT block and making decisions regarding whether to continue processing or to exit early. This decision-making process is based on predefined criteria, specifically the cumulative exiting score exceeding a certain threshold. By exiting early for simpler inputs and reserving computational resources for more complex ones, the module optimizes the overall efficiency of the tracking system. While the primary objective of the DEEM is to improve inference efficiency, it achieves this with minimal impact on tracking performance. The module is designed to ensure that early exits occur only when appropriate, thereby maintaining the accuracy and reliability of the tracking predictions. This balance between efficiency and performance is essential in real-time UAV tracking systems.

The DEEM is accomplished by employing a linear layer in conjunction with a non-linear activation function, with a slice of all tokens representing both the target template and the search image as its input, as illustrated in Fig. 3.

Its output represents the exiting score at the corresponding ViT block (layer). Specifically, take the  $i$ -th ( $i > n_{enf}$ ) layer for example, the slice of all tokens output by the  $(i - 1)$ -th ViT block is denoted by  $\mathbf{e}_1^T \mathbf{t}_{1:\mathcal{K}}^{i-1}(Z, X) := \mathbf{b}^{i-1} \in \mathbb{R}^{\mathcal{K}}$ , where  $\mathbf{e}_1^T = [1, 0, \dots, 0] \in \mathbb{R}^{\mathcal{K}}$  is a standard unit vector in  $\mathbb{R}^{\mathcal{K}}$ , the linear layer is denoted by  $\mathbf{l}^i$ , where  $d$  is the token dimension. Formally, the DEEM at layer  $i$  is defined by  $\mathbf{e}^i = \sigma(\mathbf{l}^i(\mathbf{b}^{i-1}))$ , where  $\mathbf{e}^i \in [0, 1]$  represents the exiting score of the  $i$ -th Transformer block,  $\sigma(x) = 1/(1 + e^{-x})$  denotes the sigmoid function. The forward pass exits if the cumulative exiting score  $q^i = \sum_{k=n_{enf}+1}^i \lambda \mathbf{e}^k$  exceeds  $1 - \epsilon$ , i.e.,  $q^i \geq 1 - \epsilon$ , where  $\epsilon$  is a small positive constant that enables early exiting after examining a single DEEM module. In our implementation, we set  $\epsilon = 0.05$ , which allows an early exit when the cumulative confidence exceeds 0.95. Note that, if  $n_{enf} = 0$ , theoretically all  $L$  blocks could be skipped simultaneously, resulting in no correlation computation between the template and search image. To prevent such an undesirable case, the first  $n_{enf} > 0$  layers are enforced without examination. This strategy is implemented to reduce computational burdens because these low-level blocks are expected in most cases, as low-level features provide foundational information upon which more complex features and representations can be built. Another extreme case is that, for any input, early exit never happens as by which the model is easier to reduce the training losses with more ViT blocks. To address this, we introduce a block sparsity loss, denoted as  $\mathcal{L}_{spar}$ , which penalizes smaller average exiting scores over all examined layers. This encourages, on average, an earlier exit during the forward pass to enhance efficiency. Let  $L_e$  be the maximum layer of examined ViT blocks, it follows that

$$L_e = \operatorname{argmin}_{n_{enf} < n \leq L} \left\{ \sum_{l=n_{enf}+1}^n \mathbf{e}^l \geq 1 - \epsilon \right\}. \quad (4)$$

The block sparsity loss is formally defined as follows:

$$\mathcal{L}_{spar} = \left\| \frac{1}{L_e - n_{enf}} \sum_{l=n_{enf}+1}^{L_e} \mathbf{e}^l - \tau \right\|^2, \quad (5)$$

where  $\tau$  is a constant used along with  $\lambda$  to control the block sparsity. We call  $\tau$  the block sparsity constant. Given  $\lambda$ , generally the larger  $\tau$  is, the more sparse the model will be.

### 3.4. Prediction Head and Training Objective

Following [26], we utilize a fully convolutional network-based prediction head  $\mathcal{C}$ , consisting of multiple Conv-BN-ReLU layers. The output tokens  $t_{\mathcal{K}_z+1:\mathcal{K}}^{L_e}$  associated with the search image are first reinterpreted into a 2D spatial feature map, which is then input to the prediction head. The head generates three outputs: a target classification score  $\mathbf{p} \in [0, 1]^{H_x/P \times W_x/P}$ , a local offset  $\mathbf{o} \in [0, 1]^{2 \times H_x/P \times W_x/P}$ , and a normalized bounding box size  $\mathbf{s} \in [0, 1]^{2 \times H_x/P \times W_x/P}$ . The highest classification score is used to estimate the coarse target position, i.e.,  $(x_c, y_c) = \operatorname{argmax}_{(x,y)} \mathbf{p}(x, y)$ , based on which the final target bounding box is determined by

$$\{(x_t, y_t); (w, h)\} = \{(x_c, y_c) + \mathbf{o}(x_c, y_c); \mathbf{s}(x_c, y_c)\}. \quad (6)$$

For the tracking task, we employ the weighted focal loss [56] for classification and a combination of  $L_1$  loss and GIoU loss [57] for bounding box regression. The overall loss function is formulated as:

$$\mathcal{L}_{overall} = \mathcal{L}_{cls} + \eta_{iou} \mathcal{L}_{iou} + \eta_{L_1} \mathcal{L}_{L_1} + \rho \mathcal{L}_{br} + \gamma \mathcal{L}_{spar} \quad (7)$$

where the constants  $\eta_{iou} = 2$  and  $\eta_{L_1} = 5$  are the same as in [26],  $\rho$  and  $\gamma$  are set to  $10^{-4}$  and  $10^3$  respectively. Our framework is trained end-to-end with the overall loss  $\mathcal{L}_{overall}$  after the pretrained weights of the ViT for image classification is loaded.

## 4. Experiments

This section provides detailed and comprehensive evaluation results of our approach across four well-known UAV tracking benchmarks: namely, UAV123 [60], UAV123@10fps [60], VisDrone2018 [59], and UAVDT [58]. A PC equipped with a NVIDIA TitanX GPU, 16GB RAM, and an i9-10850K CPU (3.6GHz) was used for all evaluation experiments. In order to provide a comprehensive evaluation, we evaluate our method against 22 lightweight SOTA trackers, which are categorized into three groups as in Aba-ViTrack [9], i.e., DCF-based, CNN-based, and ViT-based methods (see Table 1), alongside 14 SOTA deep trackers tailored for generic visual tracking (refer to Table 2). Note that in our study, "light trackers" and "efficient trackers" are used interchangeably to refer to trackers that prioritize low computational complexity and reduced memory usage, typically designed for environments with limited resources or real-time applications.

Table 1: Comparison of precision (Prec.) and success rate (Succ.) between BDTrack and lightweight trackers on four UAV tracking benchmarks, namely UAVDT [58], VisDrone2018 [59], UAV123 [60], and UAV123@10fps [60]. Red, blue and green indicate the first, second and third place. It is worth noting that the percent symbol (%) has been omitted for Prec. and Succ. values.

	Method	Source	UAVDT		VisDrone2018		UAV123		UAV123@10fps		Avg.	
			Prec.	Succ.	Prec.	Succ.	Prec.	Succ.	Prec.	Succ.	Prec.	Succ.
DCF-based	KCF [22]	TPAMI 15	57.1	29.0	68.5	41.3	52.3	33.1	40.6	26.5	54.6	32.5
	fDSST [61]	TPAMI 17	66.6	38.3	69.8	51.0	58.3	40.5	51.6	37.9	61.6	41.9
	BACF [62]	ICCV 17	68.6	43.2	77.4	56.7	66.0	45.9	57.2	41.3	67.3	46.8
	ECO_HC [63]	CVPR 17	69.4	41.6	80.8	58.1	71.0	49.6	64.0	46.8	71.3	49.0
	MCCCT_H [64]	CVPR 18	66.8	40.2	80.3	56.7	65.9	45.7	59.6	43.4	68.2	46.5
	ARCF [23]	ICCV 19	72.0	45.8	79.7	58.4	67.1	46.8	66.6	47.3	71.4	49.6
	AutoTrack [24]	CVPR 20	71.8	45.0	78.8	57.3	68.9	47.2	67.1	47.7	71.7	49.3
	RACF [21]	PR 20	77.3	49.4	83.4	60.0	70.2	47.7	69.4	48.6	75.1	51.4
CNN-based	HiFT [7]	ICCV 21	65.2	47.5	71.9	52.6	78.7	59.0	74.9	57.0	72.7	54.0
	SiamAPN++ [17]	IROS 21	76.9	55.6	73.5	53.2	76.8	58.2	76.4	58.1	75.9	56.3
	LightTrack [65]	CVPR 21	80.4	61.2	74.8	56.8	78.3	62.7	75.1	59.9	77.2	60.2
	TCTrack [8]	CVPR 22	69.1	50.4	77.6	57.7	77.3	60.4	75.1	58.8	74.7	56.8
	TCTrack++ [66]	TPAMI 23	72.5	53.2	80.8	60.3	74.4	58.8	78.2	60.1	76.5	58.1
	SGDViT [67]	ICRA 23	65.7	48.0	72.1	52.1	75.4	57.5	<b>86.3</b>	<b>66.1</b>	74.9	55.9
	ABDNet [44]	RAL 23	75.5	55.3	75.0	57.2	79.3	60.7	77.3	59.1	76.8	58.1
	DRCI [68]	ICME 23	<b>83.0</b>	<b>59.0</b>	83.4	60.0	76.7	59.7	73.6	55.2	79.2	58.5
PRL-Track [69]	IROS 24	73.1	53.5	72.6	53.8	79.1	59.3	74.1	58.6	74.7	56.3	
ViT-based	Aba-ViTrack [9]	ICCV 23	<b>83.4</b>	<b>59.9</b>	<b>86.1</b>	<b>65.3</b>	<b>86.4</b>	<b>66.4</b>	<b>85.0</b>	<b>65.5</b>	<b>85.2</b>	<b>64.3</b>
	LiteTrack [70]	ICRA 24	81.6	59.3	79.7	61.4	<b>84.2</b>	65.9	83.1	65.0	82.2	62.9
	SMAT [71]	WACV 24	80.8	58.7	82.5	63.4	81.8	64.6	80.4	63.5	81.4	62.6
	LightFC [72]	KBS 24	83.4	60.6	82.7	62.8	<b>84.2</b>	65.5	81.3	63.7	82.9	63.1
	AVTrack-DeiT [73]	ICML 24	82.1	58.7	<b>86.0</b>	<b>65.3</b>	<b>84.8</b>	<b>66.8</b>	83.2	<b>65.8</b>	<b>84.0</b>	<b>64.1</b>
	BDTrack-ViT	Ours	78.9	57.3	83.9	63.6	83.5	65.5	<b>84.1</b>	<b>66.1</b>	82.6	63.1
BDTrack-DeiT		<b>84.1</b>	<b>61.0</b>	<b>85.2</b>	<b>64.3</b>	<b>84.8</b>	<b>66.7</b>	83.5	65.9	<b>84.4</b>	<b>64.5</b>	

#### 4.1. Implementation Details

We employed three efficient ViT models, i.e., ViT-tiny [74] and DeiT-tiny [75], as the backbones to develop three distinct trackers, named BDTrack-ViT, BDTrack-DeiT, and BDTrack-T2T, respectively. The sizes of the search region and template are set to  $256^2$  and  $128^2$ . The head architecture, training data, hyperparameters, and training pipeline adhere to the specifications outlined in Aba-ViTrack [9]. And we apply Hanning window penalties during inference to integrate positional priors in tracking, following established practices [76].

#### 4.2. Comparison with Lightweight Trackers

In this section, we comprehensively evaluate BDTrack’s performance by comparing it with 22 SOTA lightweight trackers across four UAV tracking benchmarks. The evaluation results are shown in Table 1. As can be seen, our BDTrack-DeiT outperforms other trackers except Aba-ViTrack on all

benchmarks, regarding average (Avg.) precision (Prec.) and success rate (Succ.). RACF [21] secures the highest Prec. and Succ. in average among DCF-based trackers, with values of 75.1% and 51.4%, respectively. Among CNN-based trackers, DRCI [68] stands out with the highest average Prec. of 79.2% and Succ. of 58.5%. However, all ViT-based trackers exhibit Avg. Prec. and Succ. exceeding 81.0% and 62.0%, respectively, obviously beating the CNN-based methods and substantially outperforming the DCF-based ones. Although Aba-ViTrack achieves the highest Avg. Prec. (85.2%), our BDTrack-DeiT ranks second with only a slight gap of 0.8%, while maintaining the best Avg. Succ. of 64.5%. Notably, BDTrack-DeiT outperforms Aba-ViTrack on the UAVDT, with a success rate improvement of over 1.0%. These results highlight the advantages of our method and justify its SOTA performance for UAV tracking.

#### 4.3. Comparison with Deep Trackers

The proposed BDTrack-DeiT is also compared with 14 SOTA deep trackers. Table 2 presents the results in terms of precision (Prec.), success rate (Succ.), and their average (Avg.). It is worth noting that most deep trackers are tailored for generic tracking scenarios without prioritizing real-time constraints. Consequently, they tend to exhibit slower tracking speeds and higher model complexity, as shown in Table 3. Our BDTrack-DeiT stands out by offering the fastest speed without compromising on high performance, showcasing its competitive edge in terms of both performance and speed. Remarkably, our method achieves third place in Avg. precision on four benchmarks while securing the second position in precision on UAVDT and VisDrone2018. This underscores the effectiveness of our approach for UAV tracking tasks and highlights that our BDTrack-DeiT is equivalent in precision to state-of-the-art deep trackers. Although other deep trackers like ROMTrack [77] and EVPTrack [78] may achieve comparable performance with ours, their GPU speeds are significantly slower. In fact, our method outperforms SeqTrack and EVPTrack by being 5 and 11 times faster, respectively. By showcasing its capability to offer high precision and speed, these results demonstrate the suitability of our approach for real-time UAV tracking applications that prioritize accuracy and efficiency.

#### 4.4. Efficiency Comparison

To highlight the efficiency of the proposed trackers compared to existing methods, Table 3 presents the floating-point operations (FLOPs), the

Table 2: Precision (Prec.) and success rate (Succ.) comparison between BDTrack-DeiT and DL-based trackers.

Tracker	Source	UAVDT		VisDrone2018		UAV123		UAV123@10fps		Avg.	
		Prec.	Succ.	Prec.	Succ.	Prec.	Succ.	Prec.	Succ.	Prec.	Succ.
PrDiMP [79]	CVPR 20	75.8	55.9	79.8	60.2	87.2	66.5	83.9	64.7	81.7	61.8
SOAT [80]	CVPR 21	82.1	60.7	76.9	59.7	82.7	64.9	85.2	65.7	81.7	62.8
AutoMatch [81]	ICCV 21	82.1	62.9	78.1	59.6	83.8	64.4	78.1	59.4	80.5	61.6
SparseTT [82]	IJCAI 22	<b>82.8</b>	<b>65.4</b>	81.4	62.1	85.4	68.8	82.2	64.9	82.9	65.3
CSWinTT [83]	CVPR 22	67.3	54.0	75.2	58.0	87.6	<b>70.5</b>	87.1	68.1	79.3	62.7
SimTrack [27]	ECCV 22	76.5	57.2	80.0	60.9	<b>88.2</b>	69.2	<b>87.5</b>	69.0	83.1	64.0
OSTrack [26]	ECCV 22	<b>85.1</b>	<b>63.4</b>	84.2	<b>64.8</b>	84.7	67.4	83.1	66.1	84.2	65.2
ZoomTrack [84]	NIPS 23	77.1	57.9	81.4	63.6	<b>88.4</b>	<b>69.6</b>	<b>88.8</b>	<b>70.0</b>	83.9	<b>65.3</b>
SeqTrack [85]	CVPR 23	78.7	58.8	83.3	64.1	86.8	68.6	85.7	68.1	83.6	64.9
MAT [86]	CVPR 23	72.9	54.8	81.6	62.2	86.7	68.3	86.9	68.5	82.0	63.5
ROMTrack [77]	ICCV 23	81.9	<b>61.6</b>	<b>86.4</b>	<b>66.7</b>	87.4	69.2	85.0	67.8	<b>85.2</b>	<b>66.3</b>
DCPT [87]	ICRA 24	76.8	56.9	83.1	64.2	85.7	68.1	86.9	<b>69.1</b>	83.1	64.5
EVPTrack [78]	AAAI 24	80.6	61.2	<b>84.5</b>	<b>65.8</b>	<b>88.9</b>	<b>70.2</b>	<b>88.7</b>	<b>70.4</b>	<b>85.7</b>	<b>66.9</b>
SuperSBT [88]	TPAMI 24	80.1	59.2	82.2	63.5	85.3	67.3	87.3	<b>69.1</b>	83.7	64.7
<b>BDTrack-DeiT</b>	<b>Ours</b>	<b>84.1</b>	61.0	<b>85.2</b>	64.3	84.8	66.7	83.5	65.9	<b>84.4</b>	64.5

number of parameters during inference (Param.), and the inference speed of our method, alongside 8 SOTA efficient lightweight trackers and 8 SOTA deep trackers. Notably, as our method and AVTrack-DeiT feature adaptive architectures, the FLOPs and Params. of them vary within a range, spanning from the minimum to the maximum values. As observed, our methods achieve significantly lower FLOPs and Params. compared to all rival trackers. Even our maximum values are lower than those of most lightweight trackers. In terms of GPU speed, BDTrack-DeiT achieves the highest performance at 283.4 FPS, followed closely by AVTrack-DeiT [73] with 253.6 FPS. As for CPU speed, our tracker exhibits real-time performance on a single CPU<sup>1</sup>. Although Aba-ViTrack [9] achieves comparable performance to BDTrack-DeiT, it exhibits significantly slower inference speed. Remarkably, BDTrack-DeiT boasts over 1.6 times the GPU speed and 1.3 times the CPU speed of Aba-ViTrack, striking a better balance between tracking precision and efficiency. On the other hand, although existing deep trackers achieve comparable performance to ours, they suffer from significantly slower speeds and higher model complexity. In contrast, our method outperforms ROMTrack [77] and EVPTrack [78] by factors of 5 and 11, respectively. These results further highlight the suitability of our approach for real-time UAV tracking applications where both

<sup>1</sup>Note that the real-time performance discussed in this paper can be generalized only to platforms similar to or more advanced than ours.

Table 3: Comparison of FLOPs, parameters (Params.), and average speed between lightweight and deep trackers on four UAV tracking benchmarks.

Method		FLOPs (G)	Params. (M)	Avg.FPS	
				GPU	CPU
Lightweight	HiFT [7]	7.2	9.9	157.6	-
	SiamAPN++ [17]	8.2	14.7	162.3	-
	TCTrack [8]	16.9	8.5	133.8	-
	SGDViT [67]	11.3	23.3	105.9	-
	PRL-Track [69]	7.4	12.1	133.2	-
	Aba-ViTrack [9]	2.4	7.9	177.8	49.7
	LiteTrack [70]	28.3	7.3	115.6	-
	AVTrack-DeiT [73]	0.97-2.4	3.5-7.9	253.6	58.8
	<b>BDTrack-DeiT(Ours)</b>	<b>1.7-2.4</b>	<b>5.8-7.9</b>	<b>283.4</b>	<b>63.2</b>
Deep	OSTrack [26]	21.5	92.1	65.4	-
	SeqTrack [85]	66.3	89.4	30.1	-
	ZoomTrack [84]	21.2	91.8	60.8	-
	MAT [86]	42.9	88.4	68.4	-
	ROMTrack [77]	34.5	92.1	50.8	-
	DCPT [87]	29.4	92.9	37.3	-
	EVPTrack [78]	65.4	73.5	24.1	-
	SuperSBT [88]	24.6	65.5	30.3	-

accuracy and efficiency are critical.

#### 4.5. Attribute-Based Evaluation

To further validate the superiority of the proposed tracker over existing UAV trackers, we evaluate the performance of BDTrack-DeiT by comparing it with 14 SOTA UAV trackers on three subsets of the UAVDT [58], including ‘Motion blur’ and ‘Camera motion’. Note that we also evaluate BDTrack-DeiT without applying the components (i.e., MBRV and DEEM), denoted as BDTrack-DeiT\* for reference. The precision and success plots are illustrated in Fig. 4. As observed, BDTrack-DeiT significantly outperforms the second tracker on ‘Motion blur’ and ‘Camera motion’, with gains of 1.2%/0.7% and 2.3%/1.8% in precision/success rate, respectively. Significantly, across all these two attributes, the incorporation of the proposed components yields a noteworthy enhancement over BDTrack-DeiT\*, with improvements of 7.0%/5.0% and 7.9%/5.5% in terms of precision and success rate. Note that ‘Camera motion’ is the factor that can contribute to motion blur in visual tracking systems. When a camera moves rapidly or changes direction suddenly, it can cause motion blur in the captured images. Therefore, this attribute-based evaluation validates, directly or indirectly, the superiority and effectiveness of the proposed method in addressing the challenges posed by motion blur.

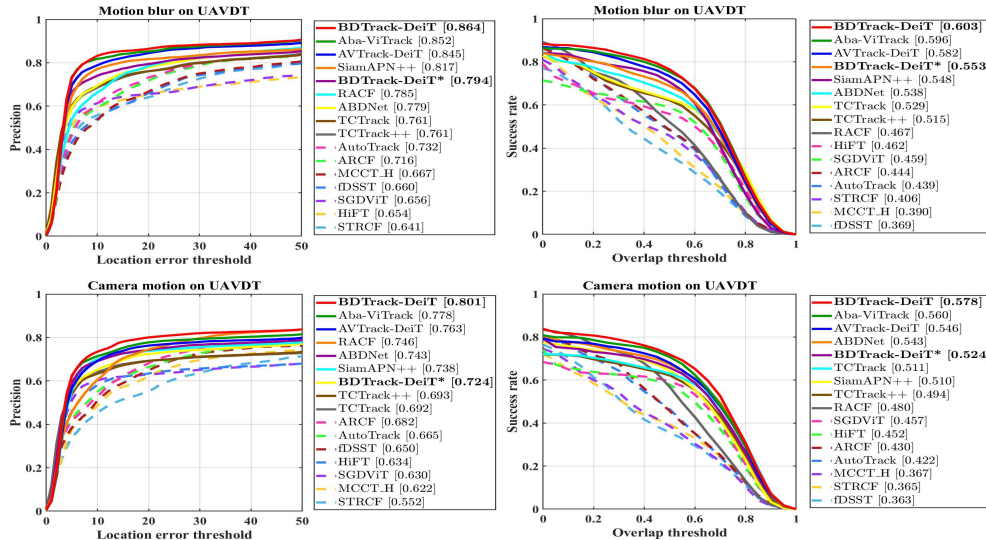


Figure 4: The precision and success plots for attribute-based comparisons on ‘Motion Blur’ (top row) and ‘Camera Motion’ (bottom row) are presented for the attribute subsets of UAVDT. Note that **BDTrack-DeiT\*** denotes **BDTrack-DeiT** without the application of the proposed components.

#### 4.6. Qualitative evaluation

Qualitative tracking results of BDTrack-DeiT and six SOTA trackers, i.e., HiFT [7], AutoTrack [24], TCTrack [8], PRL-Track [69], AVTrack-DeiT [73], and Aba-ViTrack [9], are presented in Fig. 5. Three video sequences from three different benchmarks are selected for demonstration: person10 from UAV123, uav0000164\_00000\_s from VisDrone2018, and S1606 from UAVDT. For better visualization, the low-resolution targets within the video frames are selectively zoomed, cropped, and placed in the upper right corner of their corresponding frames for display. As observed, our tracker can successfully track the targets in all challenging examples, featuring camera motion (i.e, in all sequences), occlusion (i.e, uav0000164\_00000\_s), and background clutter (i.e, S1606). Our method not only exhibits superior performance but also delivers more visually pleasing results in these scenarios, further validating the effectiveness of the proposed method for UAV tracking.

#### 4.7. Ablation Study

##### 4.7.1. Impact of learning blur robust ViTs with dynamic early exit

We add the proposed components MBRV and DEEM into the baselines one by one to evaluate their effectiveness. The evaluation results on three

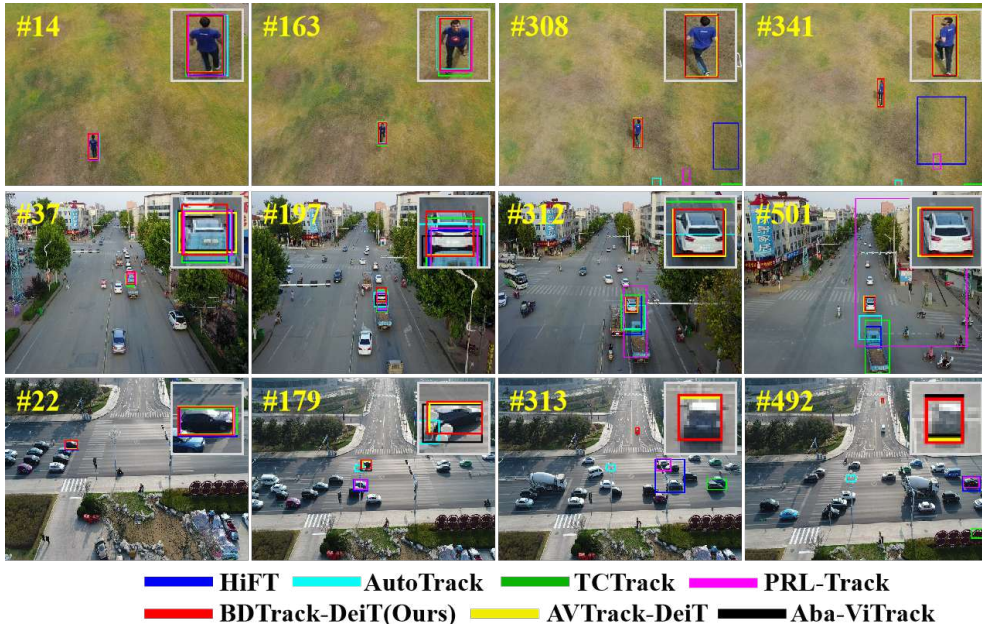


Figure 5: Visualization of qualitative comparisons between our tracker and six SOTA UAV trackers on three sequences from UAV123 [60], VisDrone2018 [59], and UAVDT [58] (i.e., person10, uav0000164\_00000\_s, and S1606).

benchmarks are shown in Table 4. As GPU speed of the baseline and its enhanced version by MBRV are theoretically equal, we provide only the speed of the baseline to eliminate potential nuances arising from randomness. As can be seen, the inclusion of MBRV leads to significant improvements in both Prec. and Succ. for the baseline tracker. Specifically, the inclusion of the MBRV leads to a significant increase of over 4.0% in average Prec. and 2.8% in average Succ. for the baseline. The improvement in performance after adding the MSE loss can be attributed to the enhanced feature consistency between clear and blurred templates. By enforcing feature similarity, the model learns more robust representations that generalize well to different blur conditions and focuses on discriminative features, leading to overall better performance beyond just handling blurred scenes. When DEEM is further integrated, consistent improvements in GPU speeds are observed, accompanied by only slight decreases in Prec. and Succ. Specifically, the GPU speeds of all baselines see increases of above 22.0%. Despite the marginal drop in Prec. and Succ. (the average drops are less than 0.6%), the overall pattern of enhanced GPU speeds and minor sacrifices in tracking performance

Table 4: Ablation study on the impact of MBRV and DEEM on the baseline tracker’s performance.

Tracker	MBVR	DEEM	UAVDT		VisDrone2018		UAV123		Avg		Avg.FPS
			Prec.	Succ.	Prec.	Succ.	Prec.	Succ.	Prec.	Succ.	
			78.6	56.7	81.6	62.2	83.7	66.1	81.3	61.7	228.7
BDTrack-DeiT	✓		<b>84.5</b>	<b>61.4</b>	<b>86.1</b>	<b>65.1</b>	<b>85.3</b>	<b>67.0</b>	<b>85.3</b>	<b>64.5</b>	-
	✓	✓	84.1	61.0	85.2	64.3	84.8	66.7	84.7	64.0	<b>279.4</b> <sub>↑22.3%</sub>

Table 5: Ablation study on the weighting of loss  $\mathcal{L}_{br}$  in training BDTrack-DeiT by varying  $\rho$  from  $0.5 \times 10^{-4}$  to  $5.0 \times 10^{-4}$ .

$\rho \times 10^{-4}$	UAVDT		VisDrone2018		UAV123		UAV123@10fps		Avg.	
	Prec.	Succ.	Prec.	Succ.	Prec.	Succ.	Prec.	Succ.	Prec.	Succ.
0.5	<b>83.4</b>	<b>60.0</b>	83.7	63.5	83.1	65.4	83.2	65.6	83.3	63.6
0.6	82.3	59.3	84.5	63.9	83.7	66.0	83.0	65.4	83.4	63.6
0.7	83.0	59.6	85.8	64.6	<b>84.1</b>	<b>66.5</b>	<b>83.3</b>	<b>66.2</b>	<b>84.0</b>	<b>64.2</b>
0.8	83.2	59.8	81.1	61.9	83.5	<b>65.8</b>	82.3	64.9	82.5	63.1
0.9	82.5	59.7	84.6	63.9	84.0	66.1	83.1	65.6	83.6	63.8
1.0	<b>84.1</b>	<b>61.0</b>	<b>85.2</b>	<b>64.3</b>	<b>84.8</b>	<b>66.7</b>	<b>83.5</b>	<b>65.9</b>	<b>84.4</b>	<b>64.5</b>
2.0	80.4	58.2	<b>86.1</b>	<b>64.8</b>	84.0	65.9	<b>84.9</b>	<b>66.5</b>	<b>83.8</b>	<b>63.8</b>
3.0	<b>83.8</b>	<b>60.7</b>	<b>85.6</b>	<b>64.5</b>	82.4	64.7	80.2	63.6	83.0	63.3
4.0	82.4	59.4	84.5	63.8	<b>84.5</b>	<b>66.5</b>	80.0	63.5	82.8	63.3
5.0	82.6	59.7	83.9	63.6	84.0	66.0	<b>82.3</b>	<b>65.1</b>	83.2	63.6

validates the effectiveness of DEEM in optimizing tracking efficiency.

#### 4.7.2. Study on weighting the loss for learning motion blur robust ViTs (MBRV)

To observe how the weight  $\rho$  of the loss  $\mathcal{L}_{br}$  influence the performance, we train BDTrack-DeiT with various  $\rho$  values ranging from  $0.5 \times 10^{-4}$  to  $5.0 \times 10^{-4}$ . The evaluation results assessed across all four datasets are shown in Table 5. Obviously, BDTrack-DeiT achieves averagely the optimal performance at  $\rho = 1.0 \times 10^{-4}$ , with 84.2% Avg. Prec. and 64.4% Avg. Succ.. Additionally, we can observe that the second and third-best performances across these datasets are scattered both above and below the value of  $1.0 \times 10^{-4}$ . These fluctuations may be attributed to the inherent differences between these datasets. When  $\rho$  is set as  $0.8 \times 10^{-4}$ , BDTrack-DeiT achieves the lowest average performance, with 82.5% Avg. Prec. and 63.1% Avg. Succ. This indicates that selecting an appropriate weight  $\rho$  is crucial for achieving optimal tracking performance. An inappropriate  $\rho$  can adversely affect the training process, leading to suboptimal results. The performance variations observed with different  $\rho$  values highlight the sensitivity of the tracking algorithm to this parameter. Therefore, careful tuning of  $\rho$  is necessary to ensure that the

Table 6: Application of our MBRV and DEEM to two SOTA trackers, with their original backbones replaced by ViT-Tiny [74] to reduce training time.

Tracker	MBVR	DEEM	UAVDT		VisDrone2018		UAV123@10fps		Avg		Avg.FPS
			Prec.	Succ.	Prec.	Succ.	Prec.	Succ.	Prec.	Succ.	
GRM [89]			78.1	56.9	85.5	64.8	82.6	65.3	82.1	62.3	218.6
	✓		<b>80.4</b>	<b>58.4</b>	<b>86.2</b>	<b>65.3</b>	<b>84.0</b>	<b>66.0</b>	<b>83.5</b>	<b>63.2</b>	-
	✓	✓	79.9	58.1	85.5	64.8	83.5	65.7	83.0	62.9	<b>257.3</b> <sub>↑17.8%</sub>
DropTrack [90]			79.4	57.5	81.9	61.8	82.5	65.1	81.3	61.5	211.4
	✓		<b>81.6</b>	<b>58.9</b>	<b>85.1</b>	<b>64.2</b>	<b>84.0</b>	<b>66.1</b>	<b>83.6</b>	<b>63.1</b>	-
	✓	✓	81.0	58.4	84.7	63.8	83.7	65.8	83.1	62.7	<b>248.6</b> <sub>↑17.5%</sub>

model performs effectively across diverse datasets and scenarios.

#### 4.7.3. Application to SOTA trackers

To demonstrate the general applicability of our approach, we integrate the proposed MBRV and DEEM into two SOTA trackers: GRM [89] and DropTrack [90]. Note that we substitute their original backbones with the tiny ViT, i.e., ViT-Tiny [74], to save training time. The evaluation results on three benchmarks are presented in Table 6. As mentioned previously, we provide only the speed of the baseline to eliminate potential nuances arising from randomness. We can observe that the inclusion of MBRV leads to noticeable improvements in both Prec. and Succ. for all baselines. Specifically, GRM and DropTrack experience increases of 1.4% and 2.3% in Avg. Prec., respectively, while their Avg. Succ. grows by 0.9% and 1.6%, respectively. When DEEM is further integrated, we consistently observe improvements in GPU speeds, along with only slight decreases in Prec. and Succ. More specifically, the GPU speeds of all baselines demonstrate increases of more than 17.0%, with tracking performance dropping by less than 0.5%. These results confirm the applicability of our method in enhancing the efficiency of existing ViT-based trackers without significantly compromising tracking performance, justifying its generality.

#### 4.7.4. Comparison with Existing Early Exit Methods

We have conducted a comparative experiments between our method and existing early exit mechanisms, including PABEE [34], ViT-EE [91], and LGViT [6]. The evaluation results are shown in Table 7. As observed, while these methods employ more complex architectures, they introduce additional complexity, struggle to balance speed and accuracy, and may exit prematurely, resulting in suboptimal performance in challenging tracking

Table 7: Comparison of performance and speed between our DEEM and various early exit methods on three UAV tracking datasets. Note that the baseline represents the enhanced tracker, which already includes the proposed MBVR.

Tracker	UAVDT		VisDrone2018		UAV123@10fps		Avg.		Avg.FPS
	Prec.	Succ.	Prec.	Succ.	Prec.	Succ.	Prec.	Succ.	
baseline	84.5	61.4	86.1	65.1	84.2	66.2	84.9	64.2	228.7
+ DEEM	<b>84.1</b>	<b>61.0</b>	<b>85.2</b>	<b>64.3</b>	<b>83.5</b>	<b>65.9</b>	<b>84.3</b>	<b>63.7</b>	279.4 $\uparrow$ 22.2%
+ PABEE [34]	81.7	58.5	<b>84.1</b>	<b>63.8</b>	82.1	63.8	82.6	62.0	<b>298.1</b> $\uparrow$ 30.7%
+ ViT-EE [91]	81.1	58.2	82.5	61.7	83.0	65.6	82.2	61.8	<b>318.7</b> $\uparrow$ 39.4%
+ LGViT [6]	<b>82.7</b>	<b>59.2</b>	83.1	62.0	<b>84.1</b>	<b>66.2</b>	<b>83.3</b>	<b>62.5</b>	264.5 $\uparrow$ 15.7%

scenarios. Specifically, although PABEE and ViT-EE achieve faster speeds than our DEEM, their performance is inferior, with an average drop of over 2.0% in precision and success rate. Additionally, while LGViT achieves relatively better performance than PABEE and ViT-EE, it comes at the cost of even slower speeds. In contrast, with the inclusion of our DEEM, the baseline’s performance drops by less than 0.6% in average precision and success rate, while achieving a speedup of over 22%. These comparisons highlight the effectiveness of the proposed DEEM in UAV tracking.

#### 4.7.5. Qualitative Results

Our BDTrack improves ViT robustness to motion blur by enforcing target feature invariance. To illustrate the effectiveness of our components, Fig.6 and Fig.7 show example attention and feature maps generated by BDTrack with and without the proposed modules (i.e., MBRV and DEEM), under motion blur conditions. For clarity, we use suffixes to indicate model variants: ‘\*’ denotes the baseline without our components, ‘+’ adds MBRV to the baseline, and ‘++’ includes both MBRV and DEEM.

*Example attention maps of the search images.* In Fig. 6, the first row shows the original search images from an example sequence (i.e., uav1 from UAV123 [60]). The images in the second, third, and fourth rows are the corresponding attention maps generated by BDTrack-DeiT\*, BDTrack-DeiT+, and BDTrack-DeiT++ (i.e., BDTrack-DeiT), respectively. As can be seen, incorporating the MBRV component (i.e., BDTrack-DeiT+) and both the MBRV and DEEM components (i.e., BDTrack-DeiT++) yields very similar results. Specifically, their visual focus on the targets is more pronounced compared to the baseline tracker (i.e., BDTrack-DeiT\*). This demonstrates that the MBRV component is able to enhance the tracker’s ability to concentrate on the target, especially under motion blur conditions, thereby improving overall tracking performance.

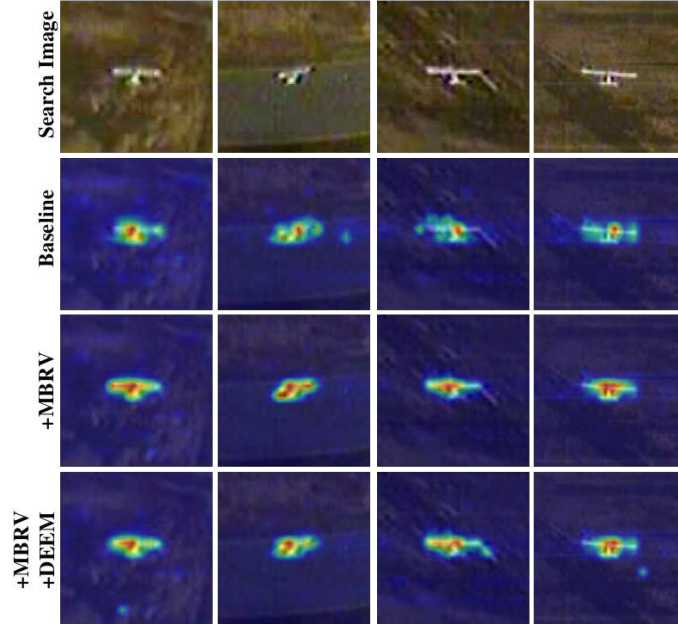


Figure 6: Visualization of attention maps. The first row displays the original search images, while the second, third, and fourth rows showcase the attention maps generated by BDTrack-DeiT without and with incorporating the proposed components.

*Example feature maps of the template images.* In each group of Fig. 7, the first row displays the original template and its blurred versions using the linear motion blur method [54] with kernel sizes 3, 5, 7 from left to right, respectively. The corresponding feature maps produced by BDTrack-DeiT\*, BDTrack-DeiT+, and BDTrack-DeiT++ are shown in the second, third, and fourth rows, respectively. This comparison provides a visual representation of the impact of the proposed MBRV and DEEM components. As can be seen, the feature maps generated by BDTrack-DeiT+ and BDTrack-DeiT++ show more consistency with changes in kernel size, whereas the feature maps from BDTrack-DeiT\* display more significant variations, especially at larger kernel sizes. These qualitative results provide visual evidence for the effectiveness of our method in learning motion blur robust feature representations with ViTs.

#### 4.8. Real-World Test

To evaluate our method’s tracking performance under real-world conditions, we conducted tests on the NVIDIA Jetson AGX Xavier 32GB, a platform well-suited for UAV applications due to its compactness and com-

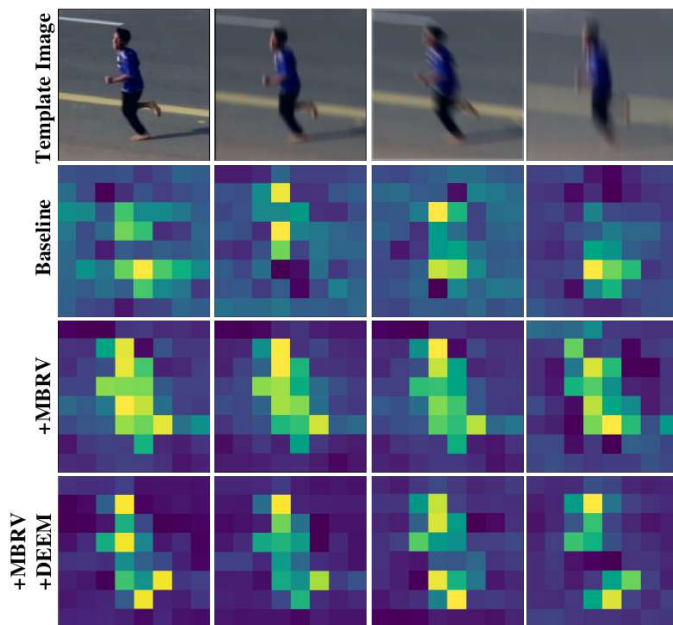


Figure 7: Visualization of feature maps. For each group, we present the original template images and their blurred versions (top row), followed by the feature maps generated by BDTrack-DeiT without (second row) and with (third and fourth rows) the proposed components. The the kernel size for linear motion blur is 3, 5 , 7, from left to right.

putational efficiency. We used the UAVTrack112\_L dataset [92] to evaluate our BDTrack-DeiT, which cover a variety of UAV scenes. Fig. 8 showcases two diverse real-world scenarios where the objects are subjected to motion blur, low resolution, fast motion challenges among others. As can be seen, our BDTrack-DeiT demonstrates robust and satisfactory performance under these challenging real-world conditions. Specifically, it maintains a center location error (CLE) of fewer than 20 pixels in all test frames, indicating high precision in tracking. Furthermore, BDTrack-DeiT consistently achieves real-time average speeds of 44 FPS. These results highlight our tracker’s robustness and efficiency, making it well-suited for UAV applications that demand high performance and speed.

## 5. Limitations and future work

### 5.1. Limitations

We present several representative failure cases in Fig. 9. Although our BDTrack demonstrates strong performance in both efficiency and motion

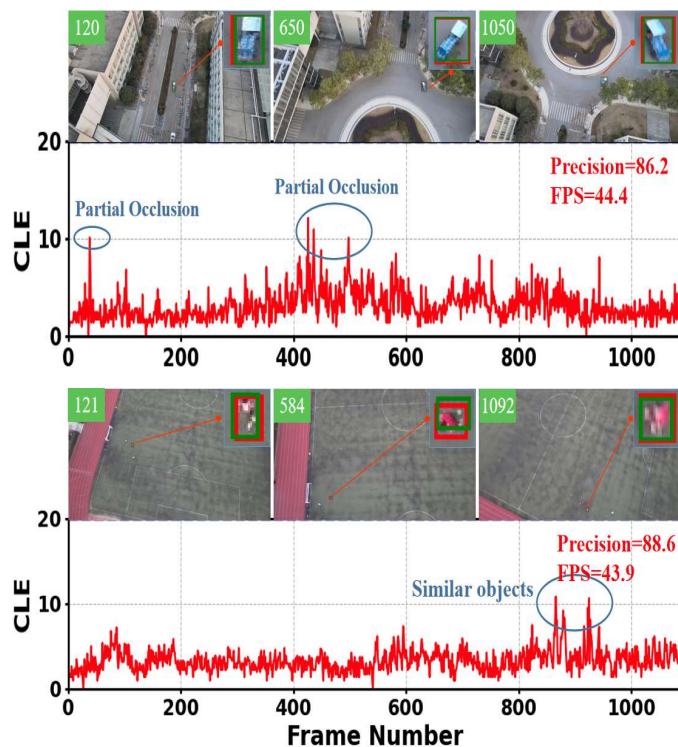


Figure 8: Real-world test on an embedded device. The CLE plots illustrate the frame-wise performance, where errors below a CLE of 20 pixels are usually considered acceptable. Note that the ground truth and tracking results are denoted by red and green boxes, respectively.

blur robustness, it still faces challenges in certain complex tracking scenarios. Specifically, the current design lacks an explicit mechanism for recovering target features after full occlusion, which may lead to identity loss or tracking failure once the target reappears (as shown in the top row). Moreover, the tracker’s performance degrades when dealing with extremely small or visually similar (as shown in the bottom row). This is primarily due to the limited spatial resolution of high-level features and the absence of fine-grained contrast enhancement, which affects the ability to distinguish the target from the background and increases the risk of drift.

### 5.2. Future work

To address these limitations, future work will focus on enhancing the tracker’s robustness in scenarios involving full occlusion and low visibility. One potential direction is to incorporate lightweight memory mechanisms that

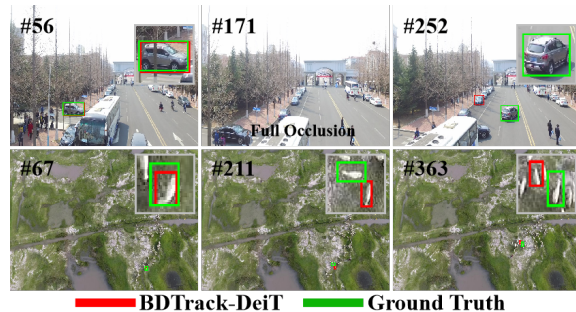


Figure 9: BDTrack limitations in complex tracking situations: Tracking errors occur when the object is fully occluded, indistinguishable from the surroundings, or occupies a very small region.

enable the tracker to re-identify the target after temporary disappearance. Additionally, we aim to improve the model’s sensitivity to fine-grained visual cues by integrating high-resolution refinement modules, thereby facilitating more accurate localization of small targets.

## 6. Conclusions

In this work, we presented a unified framework that explores both efficiency and motion blur robustness for real-time UAV tracking with Vision Transformers (ViTs). Our design introduces an adaptive computation paradigm via a dynamic early exiting mechanism, significantly reducing inference cost without compromising accuracy. Furthermore, we proposed a motion blur robust learning strategy that enforces feature invariance between clear and blurred templates, enhancing the tracker’s robustness under adverse conditions.

Extensive experiments conducted on four UAV tracking benchmarks demonstrate the effectiveness and versatility of our approach. In particular, BDTrack-DeiT achieves a more favorable speed-accuracy trade-off compared to existing state-of-the-art trackers. It outperforms lightweight models such as Aba-ViTrack [9], running approximately 1.6 times faster on GPU and 1.3 times faster on CPU, and surpasses deeper models like ROMTrack [77] and EVPTrack [78] with speed improvements of about 5 and 11 times, respectively, while achieving comparable or even better accuracy. The experimental results demonstrate that our BDTrack-DeiT achieves state-of-the-art performance in real-time UAV tracking.

## References

- [1] S.-B. Guo, Y. Meng, L. Lin, Z.-Z. Zhou, H.-L. Li, X.-P. Tian, and W.-J. Huang, “Artificial intelligence alphafold model for molecular biology and drug discovery: a machine-learning-driven informatics investigation,” *Molecular Cancer*, vol. 23, no. 1, p. 223, 2024.
- [2] S.-B. Guo, X.-Y. Cai, Y. Meng, W.-J. Huang, and X.-P. Tian, “Ai model using clinical images for genomic prediction and tailored treatment in patients with cancer,” *The Lancet. Oncology*, vol. 26, no. 3, p. e126, 2025.
- [3] H. Liu, C. Li, Q. Wu, and Y. J. Lee, “Visual instruction tuning,” *Advances in neural information processing systems*, vol. 36, pp. 34 892–34 916, 2023.
- [4] P. Xu, X. Zhu, and D. A. Clifton, “Multimodal learning with transformers: A survey,” *IEEE Transactions on Pattern Analysis and Machine Intelligence*, vol. 45, no. 10, pp. 12 113–12 132, 2023.
- [5] S. Tang and et al, “You need multiple exiting: Dynamic early exiting for accelerating unified vision language model,” *CVPR*, pp. 10 781–10 791, 2022. [Online]. Available: <https://api.semanticscholar.org/CorpusID:253734782>
- [6] G. Xu, J. Hao, and et al, “Lgvit: Dynamic early exiting for accelerating vision transformer,” *ACM Multimedia*, 2023. [Online]. Available: <https://api.semanticscholar.org/CorpusID:260350893>
- [7] Z. Cao, C. Fu, and et al, “Hift: Hierarchical feature transformer for aerial tracking,” in *ICCV*, 2021, pp. 15 457–15 466.
- [8] Z. Cao, Z. Huang, and et al, “Tctrack: Temporal contexts for aerial tracking,” in *CVPR*, 2022, pp. 14 798–14 808.
- [9] S. Li, Y. Yang, and et al, “Adaptive and background-aware vision transformer for real-time uav tracking,” in *ICCV*, 2023, pp. 13 989–14 000.
- [10] N. G. El Sayed, A. M. Yousef, G. El-Saady, M. D. Alanazi, H. A. Ziedan, and M. Abdelsattar, “Artificial intelligent fuzzy control and lapo algorithm for enhancement lvrt and power quality of grid connected pv/wind hybrid systems,” *Scientific Reports*, vol. 14, no. 1, p. 30475, 2024.

- [11] I. Y. Fawzy, Y. Mohamad, E. Shehata, and M. Abd El Sattar, "A modified perturb and observe technique for mppt of intgrated pv system using dc-dc boost converter," *Journal of Advanced Engineering Trends*, vol. 40, no. 1, pp. 63–77, 2021.
- [12] A. F. Abulkhair, M. Abdelsattar, and H. A. Mohamed, "Negative effects and processing methods review of renewable energy sources on modern power system: A review," *International Journal of Renewable Energy Research (IJRER)*, vol. 14, no. 2, pp. 385–394, 2024.
- [13] M. Abdelsattar, M. A. Ismeil, M. A. Azim, A. Abdelmoety, and A. Emad-Eldeen, "Assessing machine learning approaches for photovoltaic energy prediction in sustainable energy systems," *IEEE Access*, 2024.
- [14] M. Abdelsattar, M. A. Ismeil, M. M. Aly, and S. S. Abu-Elwfa, "Energy management of microgrid with renewable energy sources: A case study in hurghada egypt," *IEEE Access*, vol. 12, pp. 19 500–19 509, 2024.
- [15] M. Abdelsattar, M. M. Aly, and S. S. Abu-Elwfa, "Overview of microgrid with renewable energy sources operation, architecture and energy management," in *2023 24th International Middle East Power System Conference (MEPCON)*. IEEE, 2023, pp. 1–6.
- [16] A. A. Z. Diab, A.-H. M. El-Sayed, H. H. Abbas, and M. A. E. Sattar, "Robust speed controller design using h<sub>∞</sub> theory for high-performance sensorless induction motor drives," *Energies*, vol. 12, no. 5, p. 961, 2019.
- [17] Z. Cao, C. Fu, J. Ye, B. Li, and Y. Li, "Siamapn++: Siamese attentional aggregation network for real-time uav tracking," in *2021 IEEE/RSJ international conference on intelligent robots and systems (IROS)*. IEEE, 2021, pp. 3086–3092.
- [18] X. Liu, T. Xu, Y. Wang, Z. Yu, X. Yuan, H. Qin, and J. Li, "Bactrack: Building appearance collection for aerial tracking," *IEEE Transactions on Circuits and Systems for Video Technology*, 2023.
- [19] X. Yuan, T. Xu, X. Liu, Y. Wang, H. Qin, Y. Fang, and J. Li, "Multi-step temporal modeling for uav tracking," *IEEE Transactions on Circuits and Systems for Video Technology*, 2024.

- [20] S. Li, X. Yang, X. Wang, D. Zeng, H. Ye, and Q. Zhao, “Learning target-aware vision transformers for real-time uav tracking,” *IEEE Transactions on Geoscience and Remote Sensing*, 2024.
- [21] S. Li, Y. Liu, and et al, “Learning residue-aware correlation filters and refining scale for real-time uav tracking,” *Pattern Recognition*, vol. 127, p. 108614, 2022.
- [22] J. F. Henriques, R. Caseiro, and et al, “High-speed tracking with kernelized correlation filters,” *TPAMI*, vol. 37, no. 3, pp. 583–596, 2015.
- [23] Z. Huang, C. Fu, Y. Li, F. Lin, and P. Lu, “Learning aberrance repressed correlation filters for real-time uav tracking,” *2019 IEEE/CVF International Conference on Computer Vision (ICCV)*, pp. 2891–2900, 2019.
- [24] Y. Li, C. Fu, and et al, “Autotrack: Towards high-performance visual tracking for uav with automatic spatio-temporal regularization,” in *CVPR*, 2020, pp. 11 923–11 932.
- [25] F. Lin, C. Fu, Y. He, F. Guo, and Q. Tang, “Learning temporary block-based bidirectional incongruity-aware correlation filters for efficient uav object tracking,” *IEEE Transactions on Circuits and Systems for Video Technology*, vol. 31, no. 6, pp. 2160–2174, 2020.
- [26] B. Ye, H. Chang, and et al, “Joint feature learning and relation modeling for tracking: A one-stream framework,” in *ECCV*. Springer, 2022, pp. 341–357.
- [27] B. Chen, P. Li, and et al, “Backbone is all your need: A simplified architecture for visual object tracking,” in *ECCV*. Springer, 2022, pp. 375–392.
- [28] F. Xie, C. Wang, and et al, “Correlation-aware deep tracking,” in *CVPR*, 2022, pp. 8751–8760.
- [29] C. Tang, X. Wang, Y. Bai, Z. Wu, J. Zhang, and Y. Huang, “Learning spatial-frequency transformer for visual object tracking,” *IEEE Transactions on Circuits and Systems for Video Technology*, vol. 33, no. 9, pp. 5102–5116, 2023.

- [30] Y. Kaya, S. Hong, and et al, “Shallow-deep networks: Understanding and mitigating network overthinking,” in *ICML*, 2018. [Online]. Available: <https://api.semanticscholar.org/CorpusID:147703951>
- [31] H. Li, H. Zhang, and et al, “Improved techniques for training adaptive deep networks,” *ICCV*, pp. 1891–1900, 2019. [Online]. Available: <https://api.semanticscholar.org/CorpusID:201070148>
- [32] Y. Liu, F. Meng, and et al, “Faster depth-adaptive transformers,” in *AAAI*, 2020. [Online]. Available: <https://api.semanticscholar.org/CorpusID:229283620>
- [33] J. Xin, R. Tang, and et al, “Berxit: Early exiting for bert with better fine-tuning and extension to regression,” in *EACL*, 2021. [Online]. Available: <https://api.semanticscholar.org/CorpusID:233189542>
- [34] W. Zhou, C. Xu, T. Ge, J. McAuley, K. Xu, and F. Wei, “Bert loses patience: Fast and robust inference with early exit,” *Advances in Neural Information Processing Systems*, vol. 33, pp. 18 330–18 341, 2020.
- [35] M. Phuong and C. H. Lampert, “Distillation-based training for multi-exit architectures,” *ICCV*, pp. 1355–1364, 2019. [Online]. Available: <https://api.semanticscholar.org/CorpusID:207994757>
- [36] S. Teerapittayanon and et al, “Branchynet: Fast inference via early exiting from deep neural networks,” *ICPR*, pp. 2464–2469, 2016. [Online]. Available: <https://api.semanticscholar.org/CorpusID:2916466>
- [37] A. Ghodrati, B. E. Bejnordi, and et al, “Frameexit: Conditional early exiting for efficient video recognition,” *CVPR*, pp. 15 603–15 613, 2021. [Online]. Available: <https://api.semanticscholar.org/CorpusID:233423498>
- [38] Z. Fei, X. Yan, and et al, “Deecap: Dynamic early exiting for efficient image captioning,” *CVPR*, pp. 12 206–12 216, 2022. [Online]. Available: <https://api.semanticscholar.org/CorpusID:249916633>
- [39] C. Fu, B. Li, and et al, “Correlation filters for unmanned aerial vehicle-based aerial tracking: A review and experimental evaluation,” *IEEE GEOSC REM SEN M*, vol. 10, pp. 125–160, 2020. [Online]. Available: <https://api.semanticscholar.org/CorpusID:235358629>

- [40] B. Ma, L. Huang, and et al, “Visual tracking under motion blur,” *TIP*, vol. 25, no. 12, pp. 5867–5876, 2016.
- [41] C. Seibold, A. Hilsmann, and et al, “Model-based motion blur estimation for the improvement of motion tracking,” *CVIU*, vol. 160, pp. 45–56, 2017.
- [42] Q. Guo, Z. Cheng, and et al, “Learning to adversarially blur visual object tracking,” in *ICCV*, 2021, pp. 10 839–10 848.
- [43] Q. Guo, W. Feng, and et al, “Effects of blur and deblurring to visual object tracking,” *arXiv preprint arXiv:1908.07904*, 2019.
- [44] H. Zuo, C. Fu, and et al, “Adversarial blur-deblur network for robust uav tracking,” *RAL*, vol. 8, no. 2, pp. 1101–1108, 2023.
- [45] J. Ding, Y. Huang, W. Liu, and K. Huang, “Severely blurred object tracking by learning deep image representations,” *IEEE Transactions on Circuits and Systems for Video Technology*, vol. 26, no. 2, pp. 319–331, 2015.
- [46] Z. Mao, X. Chen, and et al, “Robust tracking for motion blur via context enhancement,” in *ICIP*. IEEE, 2021, pp. 659–663.
- [47] L. Yang, S. Gu, C. Shen, X. Zhao, and Q. Hu, “Skeleton neural networks via low-rank guided filter pruning,” *IEEE Transactions on Circuits and Systems for Video Technology*, vol. 33, no. 12, pp. 7197–7211, 2023.
- [48] J. Mao, H. Yang, and et al, “Tprune: Efficient transformer pruning for mobile devices,” *ACM Trans. Cyber Phys. Syst.*, vol. 5, pp. 26:1–26:22, 2021.
- [49] Y. Li, G. Yuan, and et al, “Efficientformer: Vision transformers at mobilenet speed,” *ArXiv*, vol. abs/2206.01191, 2022.
- [50] Y. Rao, W. Zhao, and et al, “Dynamicvit: Efficient vision transformers with dynamic token sparsification,” in *NeurIPS*, 2021.
- [51] H. Yin, Vahdat, and et al, “A-vit: Adaptive tokens for efficient vision transformer,” in *CVPR*, 2022, pp. 10 809–10 818.

- [52] J. Sivertsen, “Similarity problems in high dimensions,” *ArXiv*, vol. abs/1906.04842, 2019. [Online]. Available: <https://api.semanticscholar.org/CorpusID:186206731>
- [53] D. Srivamsi, O. M. Deepak, and et al, “Cosine similarity based word2vec model for biomedical data analysis,” *ICOEI*, pp. 1400–1404, 2023. [Online]. Available: <https://api.semanticscholar.org/CorpusID:258869989>
- [54] D. Dwibedi, I. Misra, and et al, “Cut, paste and learn: Surprisingly easy synthesis for instance detection,” *ICCV*, pp. 1310–1319, 2017. [Online]. Available: <https://api.semanticscholar.org/CorpusID:2229234>
- [55] T. Askari, H. Hassanpour, and Javaran, “Retracted: Using a blur metric to estimate linear motion blur parameters,” 2023. [Online]. Available: <https://api.semanticscholar.org/CorpusID:266073671>
- [56] H. Law and J. Deng, “Cornernet: Detecting objects as paired keypoints,” *IJCV*, vol. 128, pp. 642–656, 2018.
- [57] S. H. Rezatofighi, N. Tsoi, J. Gwak, A. Sadeghian, I. D. Reid, and S. Savarese, “Generalized intersection over union: A metric and a loss for bounding box regression,” *CVPR*, pp. 658–666, 2019.
- [58] D. Du, Y. Qi, and et al, “The unmanned aerial vehicle benchmark: Object detection and tracking,” in *ECCV*, 2018, pp. 370–386.
- [59] L. Wen, P. Zhu, and et al, “Visdrone-sot2018: The vision meets drone single-object tracking challenge results,” in *ECCV*, 2018, pp. 0–0.
- [60] M. Mueller, N. Smith, and et al, “A benchmark and simulator for uav tracking,” in *ECCV*. Springer, 2016, pp. 445–461.
- [61] M. Danelljan, G. Häger, and et al, “Discriminative scale space tracking,” *PAMI*, vol. 39, no. 8, pp. 1561–1575, 2017.
- [62] H. Kiani Galoogahi, A. Fagg, and S. Lucey, “Learning background-aware correlation filters for visual tracking,” in *Proceedings of the IEEE international conference on computer vision*, 2017, pp. 1135–1143.
- [63] M. Danelljan, G. Bhat, F. S. Khan, and M. Felsberg, “Eco: Efficient convolution operators for tracking,” *2017 IEEE Conference on Computer Vision and Pattern Recognition (CVPR)*, pp. 6931–6939, 2017.

- [64] N. Wang, W. Zhou, and et al, “Multi-cue correlation filters for robust visual tracking,” in *CVPR*, 2018, pp. 4844–4853.
- [65] B. Yan, H. Peng, K. Wu, D. Wang, J. Fu, and H. Lu, “Lighttrack: Finding lightweight neural networks for object tracking via one-shot architecture search,” *2021 IEEE/CVF Conference on Computer Vision and Pattern Recognition (CVPR)*, pp. 15 175–15 184, 2021.
- [66] Z. Cao, Z. Huang, L. Pan, S. Zhang, Z. Liu, and C. Fu, “Towards real-world visual tracking with temporal contexts,” *IEEE Transactions on Pattern Analysis and Machine Intelligence*, 2023.
- [67] L. Yao, C. Fu, and et al, “Sgdvit: Saliency-guided dynamic vision transformer for uav tracking,” *arXiv preprint arXiv:2303.04378*, 2023.
- [68] D. Zeng, M. Zou, and et al, “Towards discriminative representations with contrastive instances for real-time uav tracking,” in *ICME*. IEEE, 2023, pp. 1349–1354.
- [69] C. Fu, X. Lei, H. Zuo, L. Yao, G. Zheng, and J. Pan, “Progressive representation learning for real-time uav tracking,” *arXiv preprint arXiv:2409.16652*, 2024.
- [70] Q. Wei, B. Zeng, J. Liu, L. He, and G. Zeng, “Litetrack: Layer pruning with asynchronous feature extraction for lightweight and efficient visual tracking,” *ArXiv*, vol. abs/2309.09249, 2023. [Online]. Available: <https://api.semanticscholar.org/CorpusID:262043880>
- [71] G. Y. Gopal and M. A. Amer, “Separable self and mixed attention transformers for efficient object tracking,” in *Proceedings of the IEEE/CVF Winter Conference on Applications of Computer Vision*, 2024, pp. 6708–6717.
- [72] Y. Li, B. Wang, X. Wu, Z. Liu, and Y. Li, “Lightweight full-convolutional siamese tracker,” *Knowl. Based Syst.*, vol. 286, p. 111439, 2024. [Online]. Available: <https://api.semanticscholar.org/CorpusID:263829668>
- [73] Y. Li, M. Liu, Y. Wu, X. Wang, X. Yang, and S. Li, “Learning adaptive and view-invariant vision transformer for real-time uav tracking,” in *Forty-first International Conference on Machine Learning*, 2024.

- [74] A. Dosovitskiy, L. Beyer, and et al, “An image is worth 16x16 words: Transformers for image recognition at scale,” *arXiv preprint arXiv:2010.11929*, 2020.
- [75] Touvron and et al, “Training data-efficient image transformers & distillation through attention,” in *ICML*. PMLR, 2021, pp. 10 347–10 357.
- [76] Z. Zhang, H. Peng, and et al, “Ocean: Object-aware anchor-free tracking,” in *ECCV*. Springer, 2020, pp. 771–787.
- [77] Y. Cai, J. Liu, and et al, “Robust object modeling for visual tracking,” in *ICCV*, 2023, pp. 9589–9600.
- [78] L. Shi, B. Zhong, Q. Liang, N. Li, S. Zhang, and X. Li, “Explicit visual prompts for visual object tracking,” in *AAAI*, 2024.
- [79] M. Danelljan, L. Gool, and et al, “Probabilistic regression for visual tracking,” in *CVPR*, 2020, pp. 7183–7192.
- [80] Z. Zhou, W. Pei, and et al, “Saliency-associated object tracking,” in *ICCV*, 2021, pp. 9866–9875.
- [81] Z. Zhang, Y. Liu, and et al, “Learn to match: Automatic matching network design for visual tracking,” in *ICCV*, 2021, pp. 13 339–13 348.
- [82] Z. Fu, Z. Fu, and et al, “Sparsett: Visual tracking with sparse transformers,” *arXiv preprint arXiv:2205.03776*, 2022.
- [83] Z. Song, J. Yu, Y.-P. P. Chen, and W. Yang, “Transformer tracking with cyclic shifting window attention,” in *Proceedings of the IEEE/CVF conference on computer vision and pattern recognition*, 2022, pp. 8791–8800.
- [84] Y. Kou, J. Gao, B. Li, G. Wang, W. Hu, Y. Wang, and L. Li, “Zoomtrack: Target-aware non-uniform resizing for efficient visual tracking,” *Advances in Neural Information Processing Systems*, vol. 36, 2023.
- [85] X. Chen, H. Peng, and et al, “Seqtrack: Sequence to sequence learning for visual object tracking,” in *CVPR*, 2023, pp. 14 572–14 581.

- [86] H. Zhao, D. Wang, and H. Lu, “Representation learning for visual object tracking by masked appearance transfer,” in *Proceedings of the IEEE/CVF Conference on Computer Vision and Pattern Recognition*, 2023, pp. 18 696–18 705.
- [87] J. Zhu, H. Tang, Z.-Q. Cheng, J.-Y. He, B. Luo, S. Qiu, S. Li, and H. Lu, “Dcpt: Darkness clue-prompted tracking in nighttime uavs,” *IEEE International Conference on Robotics and Automation (ICRA)*, 2024.
- [88] F. Xie, W. Yang, C. Wang, L. Chu, Y. Cao, C. Ma, and W. Zeng, “Correlation-embedded transformer tracking: A single-branch framework,” *arXiv preprint arXiv:2401.12743*, 2024.
- [89] S. Gao, C. Zhou, and et al, “Generalized relation modeling for transformer tracking,” in *CVPR*, 2023, pp. 18 686–18 695.
- [90] Q. Wu, T. Yang, and et al, “Dropmae: Masked autoencoders with spatial-attention dropout for tracking tasks,” in *CVPR*, 2023, pp. 14 561–14 571.
- [91] A. Bakhtiarnia, Q. Zhang, and A. Iosifidis, “Multi-exit vision transformer for dynamic inference,” *arXiv preprint arXiv:2106.15183*, 2021.
- [92] C. Fu, Z. Cao, Y. Li, J. Ye, and C. Feng, “Onboard real-time aerial tracking with efficient siamese anchor proposal network,” *IEEE Transactions on Geoscience and Remote Sensing*, vol. 60, pp. 1–13, 2021.